Sponsored by—
American Institute of Aeronautics and Astronautics (AIAA)
American Astronautical Society (AAS)

78-1399

Dynamical Characteristics Associated with Deploying, Orbiting, Beam-Type Appendages

K. W. Lips and V. J. Modi, *University of British Columbia, Vancouver, Canada*

AIAA/AAS ASTRODYNAMICS CONFERENCE

Palo Alto, Calif./August 7-9, 1978

DYNAMICAL CHARACTERISTICS ASSOCIATED WITH DEPLOYING, ORBITING, BEAM-TYPE APPENDAGES†

K.W. Lips* and V.J. Modi**
Department of Mechanical Engineering
The University of British Columbia
Vancouver, B.C., Canada V6T 1W5

Abstract

Investigated are vibration characteristics associated with a beam-type spacecraft appendage which is not only deploying and rotating but, in addition, is moving along an arbitrary orbit. Linear equations governing in-plane and out-of-plane vibration are derived by following a Lagrangian procedure. The second order kinetic-potential used is discretized by expanding elastic displacements in terms of a suitable set of admissible functions. Axial foreshortening associated with transverse displacement is included in the analysis. Instantaneous eigenvalues and eigenfunctions are solved for over a large range of system parameters. As well, representative response data is presented based on direct numerical integration of the equations. Effects of deployment are isolated and illustrated together with the relatively strong stiffening influence of the spin parameter. Although deployment rate tends to introduce instability, it is the deployment-related Coriolis loading which can result in excessive displacements should deployment times be too long. Another result of interest is the fact that an orbiting beam can have higher characteristic frequencies associated with it than a beam spinning but not orbiting. Overall such information should be of particular value when considering interactions among the structural, control, and vehicle dynamics.

Nomenclature

[A]	known constant matrix dependent on choice of admissible functions - see equation (2b)
c.m.	instantaneous centre of mass of overall spacecraft - Figure 1.
c(),s()	cosine(), sine(), respectively
[C]	known constant matrix dependent on choice of admissible functions - see equation (2b)
dm	mass element of appendage - Figure 1
D	spatial domain of appendage
[D]	known constant matrix dependent on choice of admissible functions - see equation (2b)
e	orbital eccentricity
E	Young's modulus of elasticity
{f}	forcing function along 'y' direction
g_m	m^{th} normal mode of simple cautilever beam
G	universal gravitational constant
[I]	unit matrix
J_{ij}	area moment of inertia of beam cross section, = J if section symmetric, material isotropic
k_m	constant of proportionality associated with m^{th} eigenvalue
[K]	matrix defined in equation (3c)
[K']	matrix defined by equations (2b)
ℓ	beam length at any given time
$\hat{\dot{\ell}}$	$\dot{\ell}/\ell$
$\hat{\ddot{\ell}}$	$\ddot{\ell}/\ell$
L	fully deployed beam length
$\tilde{L}$	Lagrangian density
$\mathcal{L}$	Lagrangian
M	mass of attracting body at 'S'
N	number of admissible functions used
q_k	k^{th} generalized coordinate
$\underline{R}_c$	radius vector locating instantaneous centre of mass of spacecraft with respect to attracting centre of force 'S'- Figure 1
S	centre of force
t	time
$\hat{t}$	$= \dot{\theta}t$, if $e \neq 0$ a mean value of $\dot{\theta}$ used
T_1'	$\Omega^2 + (\frac{1}{2} + \frac{3}{2}\,c2\Phi)/(1 + ec\theta)$
T_3'	$(\frac{1}{2} + \frac{3}{2}\,c2\Phi)/(1 + ec\theta)$
T_4'	$\ddot{\Omega} + (\frac{3}{2}\,s2\Phi)/(1 + ec\theta)$
T_5'	$(\frac{1}{2} - \frac{3}{2}\,c2\Phi)/(1 + ec\theta)$
v(x,t), w(x,t)	elastic displacements of dm measured along the y,z directions of the appendage, respectively
$\hat{v},\hat{w}$	$= v/\ell,\ w/\ell$
$\hat{x}$	$= x/\ell$, nondimensional location along the beam
x,y,z	right hand, orthogonal, body-fixed coordinate system with orgin at c.m. as in Figure 1
X_0,Y_0,Z_0	orbiting reference frame with origin at c.m.; X_0 along local vertical, Y_0 along tangent to orbit, and Z_0 parallel to orbit normal
β_m^4	frequency parameter associated with m^{th} eigenvalue, $= \rho\omega_m^2\ell^4/EJ$
βm_i	frequency parameter for in-plane vibration
βm_o	frequency parameter for out-of-plane vibration
ξ_m	m^{th} generalized coordinate for in-plane vibration
ζ_m	m^{th} generalized coordinate for out-of-plane vibration
$\varepsilon_m,\varepsilon_m^*$	complex conjugate pair of eigenfunctions
θ	true anomaly
λ_a	deployment acceleration parameter, $\rho\ddot{\ell}\ell^4/EJ$
λ_r	deployment rate parameter, $\rho\hat{\dot{\ell}}^2\ell^4/EJ$
λ_s	spin parameter, $\rho\Omega^2\ell^4/EJ$
μ	gravitational constant = GM
$\rho(x)$	linear mass density of beam
σ_m	constant associated with m^{th} eigenvalue of simple cantilever beam
Φ	planar pitch libration of xy axes in the orbital plane

†Supported by the National Research Council of Canada, Grant No. A-2181

*Graduate Research Assistant, Member AIAA
**Professor, Member AIAA

ω_m	natural frequency of the m^{th} eigenfunction of a simple cantilever beam
$\dot{\Omega}$	$= \dot{\Phi} + \dot{\theta}$, total spin rate
[ ]	square matrix
{ }	column matrix

Dots and primes indicate derivatives with respect to time $(t,\hat{t})$ and space $(x,\hat{x})$ respectively

1. Introduction

Early in the history of artificial earth satellites relatively long flexible beam-like structures were adopted to fill a variety of roles, e.g., placement of experimental packages, communication antennae, gravity-gradient stabilizing booms, etc. This initial use of flexibility has been extended and continues to the present day while promising to become even more pervasive in the future. As examples one can point to the Communications Technology Satellite (CTS/Hermes), American Space Shuttle, the Orbiting Solar Observatory (OSO), MARINER-4, and INTELSAT V. Essential to the analysis and control of attitude motions of these spacecraft are dynamical characteristics associated with flexible members. Of course, this is even more critical for very large flexible assemblies such as the proposed Space Station, Solar Sail, and Solar Satellite Power Station (SSPS).

To date, considerable effort has been applied toward understanding behaviour of flexible members themselves in order to examine any effects they might have on overall steady-state librational motions.[1] Reference 2 reviews and comments on methods for dealing with a rotating beam only. The problem becomes more complex if one wishes to examine transient behaviour during attitude acquisition when appendanges can be continuously extending and rotational velocities can be relatively high. Such deployment results in time-varying spacecraft inertias while fundamental vibration characteristics of the appendages also become functions of time. Some work has been initiated for extending beams which are not rotating and are not in orbit.[3,4] The purpose of this paper is to investigate the dynamics of a beam-type appendage which is not only deploying and rotating but, in addition, is following an arbitrary trajectory.

Reference 5 presents nonlinear partial differential equations only, for the transverse vibrations of a deploying beam having variable stiffness and density, appended to a spacecraft, immersed in the gravitational field, and undergoing planar libration. Also presented are some preliminary results for linear in-plane vibration characteristics. In the current paper use is made of a somewhat simplified model - a 'uniform' beam undergoing linear motions only. The ordinary differential equations governing in-plane and out-of-plane oscillations are more efficiently derived by non-dimensionalizing and discretizing the second order Lagrangian prior to application of the Lagrange equation. Deployment rate and angular velocity are permitted to vary with time. Axial foreshortening of the beam associated with transverse displacements is also incorporated into the analysis. The resulting linear equations themselves are presented along with a comprehensive look at the impact deployment and rotation can have on the fundamental vibration characteristics as well as on response in-plane and out-of-plane. Aside from the large number of variables involved, the equations are difficult to solve in general due to their coupled, non-autonomous nature. An approach implemented here is to treat a truncated set of the equations as a discrete eigenvalue problem at any given instant during deployment. Eigenvalues and eigenfunctions are then solved for over a large range of parameters.

Discussion

Use of what is essentially the Assumed-Mode approach provides a rigorous basis for evaluating system response. However it depends on a knowledge of model characteristics which are time variable. The instantaneous characteristics found here are valid only over that instant of time for which the coefficients - Eq. (3) - can be considered constants. Consequently model data must be continually updated as in the 'quasi-model' approach of Cherchas.[7] This tends to eliminate the classical advantage of eigenvalue analysis - invariance with time. The approach adopted here is to make use of the eigenvalue analysis only to assess fundamental vibration characteristics and their variation. Response is then based on a direct numerical integration of generalized coordinate equations.

Additional assumptions which lead to closed-form solutions of the equations of motion are also explored.

2. General Equations

Derivation

Figure 1 depicts the essential elements of the system studied - a cantilevered slender beam-type appendage deploying in a spin plane which coincides with the orbital plane. Vibration consists of small oscillations in the plane and out of the plane of rotation. Note that the beam is just one element of an overall spacecraft system whose instantaneous centre of mass is in orbit at a distance, Rc from the attracting centre 'S'. X_0 lies along the local vertical. Φ measures the planar libration of the body-fixed x axis with respect to the orbiting X_0 axis. When undeflected, the location of the beam coincides with the x axis. Deployment $(\dot{\ell})$ occurs along the local axial direction. Offset of the cantilevered end from the centre of mass is neglected. Also, linear density ρ and stiffness terms EJ are considered constant.

Linear stress/strain relations are assumed. However, geometric nonlinearity must be taken into account to yield linear vibration equations.[6] That is, axial foreshortening due to transverse oscillation must be allowed for to reflect the effect of axial tension.

Mass element dm (Fig. 1) derives kinetic energy from rotation, flexure, and deployment. In addition, it has elastic and gravitational potential energies. Integration of the kinetic-potential over the entire length of the beam, retaining all terms up to second order, yields the desired Lagrangian:

$$\mathcal{L} = \int_D \tilde{L}\, dD = \int_0^{\ell} \left\{ \frac{\rho}{2}(\dot{v}^2+\dot{w}^2) + \rho\dot{\ell}(\dot{v}v'+\dot{w}w') - \frac{E}{2}\left(J_{zz}v''^2 + J_{yy}w''^2 \right) \right.$$

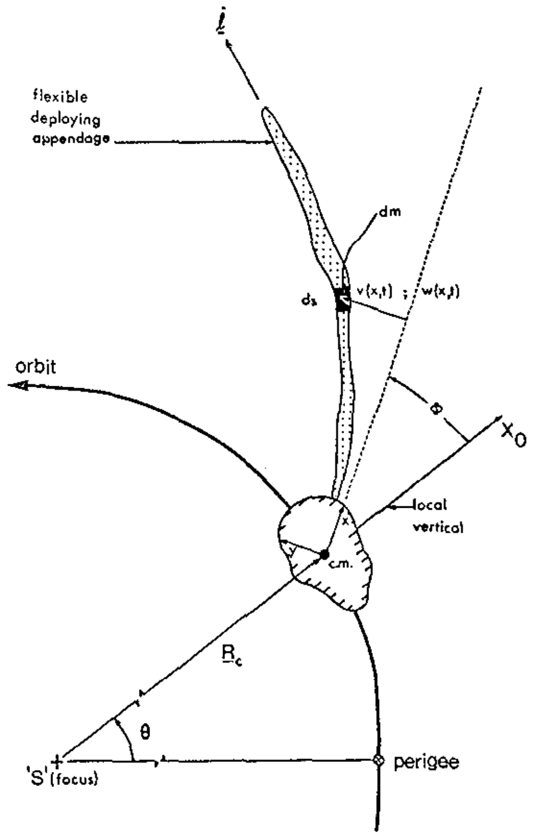

Fig. 1 Model of deploying, orbiting, librating, beam-type appendage experiencing flexural oscillation both in the plane of rotation [v(x,t)] and out of the plane of rotation [w(x,t)].

$$- \rho\left\{\left[\dot{\Omega}^2+\left(\frac{\mu}{R_c^3}\right)\left(\frac{1}{2}+\frac{3}{2}\,c2\Phi\right)\right]\left(\frac{\ell^2-x^2}{2}\right)-\ddot{\ell}(\ell-x)-\dot{\ell}^2\right\}\left(\frac{v'^2+w'^2}{2}\right)$$

$$+ \rho\left[\dot{\Omega}^2+\left(\frac{\mu}{R_c^3}\right)\left(\frac{1}{2}-\frac{3}{2}\,c2\Phi\right)\right]\frac{v^2}{2}$$

$$+ \rho\left(\frac{\mu}{R_c^3}\right)\left(\frac{1}{2}-\frac{3}{2}\,c2\Phi\right)\frac{w^2}{2}$$

$$- \rho\left[\ddot{\Omega}x + 2\dot{\Omega}\dot{\ell} + \left(\frac{3}{2}\right)\left(\frac{\mu}{R_c^3}\right)x\,s2\Phi\right]v$$

$$+ \frac{\rho}{2}\left(\frac{\mu}{R_c^3}\right)\left(\frac{1}{2}+\frac{3}{2}\,c2\Phi\right)x^2\Bigg]dx \qquad (1)$$

Nondimensionalize using,

$$\hat{v} = v/\ell;\ \hat{w} = w/\ell;\ \hat{x} = x/\ell;\ \hat{t} = \dot{\theta}t;$$

$$\hat{\ell} = \frac{1}{\ell}\frac{\delta\ell}{\delta\hat{t}}$$

where, $\dot{\theta}$ ~ mean orbital rate.

Also, introduce the cantilever modes of simple flexure $[g_m(\hat{x})]$ as a suitable set of admissible functions so that,

$$\hat{v}(\hat{x},\hat{t}) = \sum_m g_m(x/\ell)\ \xi_m(\hat{t})$$

$$\hat{w}(\hat{x},\hat{t}) = \sum_m g_m(x/\ell)\ \zeta_m(\hat{t})$$

Substituting into (1), completing the integration, and introducing matrix notation yields the discretized Lagrangian to second order:

$$\mathcal{L} = \frac{\rho}{2}\dot{\theta}^2\ell^3\Big[\{\dot{\xi}\}^T[I]\{\dot{\xi}\} + \{\dot{\zeta}\}^T[I]\{\dot{\zeta}\}$$

$$+ 2\hat{\ell}\{\dot{\xi}\}^T([I]+[A])\{\xi\} + 2\hat{\ell}\{\dot{\zeta}\}^T([I]+[A])\{\zeta\}$$

$$+ \{\xi\}^T(\hat{\Omega}^2[I]+[K'])\{\xi\} + \{\zeta\}^T[K']\{\zeta\}$$

$$- \frac{4}{\beta_m}\left(2\sigma_m\hat{\Omega}\hat{\ell} + \frac{T_4'}{\beta_m}\right)\{\xi\} + \frac{T_3'}{3}\hat{x}^3\Big] \qquad (2a)$$

where, $J_{yy} = J_{zz} = J$

$$\int_0^1 g_m g_n\, d\hat{x} = \delta_{mn} = [I] \text{ - symmetric}$$

$$\int_0^1 g_m(1-\hat{x})\ g_n'\, d\hat{x} = A_{mn} = [A] \text{ - skew-symmetric}$$

$$\int_0^1 g_m'(1-\hat{x}^2)\ g_n'\, d\hat{x} = C_{mn} = [C] \text{ - symmetric}$$

$$\int_0^1 g_m'(1-\hat{x})\ g_n'\, d\hat{x} = D_{mn} = [D] \text{ - symmetric}$$

$$[K'] = (2[D] - 2[A] - [C])\hat{\ell}^2 + [D]\hat{\hat{\ell}}$$

$$- [C]\frac{T_1'}{2} + [I](T_5'+\hat{\ell}^2-\hat{\omega}_m^2)$$

$$T_1' = \dot{\Omega}^2 + \frac{\left(\frac{1}{2}+\frac{3}{2}\,c2\Phi\right)}{1+ec\theta}$$

$$T_3' = \frac{\frac{1}{2}+\frac{3}{2}\,c2\Phi}{1+ec\theta}$$

$$T_4' = \ddot{\Omega} + \frac{\frac{3}{2}\,s2\Phi}{1+ec\theta}$$

$$T_5' = \frac{\frac{1}{2}-\frac{3}{2}\,c2\Phi}{1+ec\theta} \qquad (2b)$$

$$\hat{\Omega} = \dot{\Phi} + \dot{\theta}$$

$$\ddot{\Omega} = \ddot{\Phi}\quad \ddot{\theta}$$

Properties of g_m include;

$$g_m^{(iv)} + \beta_m^4\, g_m = 0$$

$$g_m(0) = g_m'(0) = g_m''(1) = g_m'''(1) = 0$$

$$\beta_m^4 = \frac{\rho}{EI}\,\omega_m^2\,\ell^2;\quad \int_0^1 g_m\, g_n d\hat{x} = \delta_{mn}$$

$$\int_0^1 g_m''\ g_n'' d\hat{x} = \beta_m\ \delta_{mn}$$

$$\sigma_m = \frac{\cosh\beta_m + \cos\beta_m^4}{\sinh\beta_m + \sin\beta_m}$$

Application of the Lagrange equations

$$\frac{d}{dt}\left\{\frac{\partial \mathcal{L}}{\partial \dot{q}_k}\right\} - \left\{\frac{\partial \mathcal{L}}{\partial q_k}\right\} = \{0\};\ q_k = \xi_k,\ \zeta_k \tag{3}$$

results in equations or motion governing generalized coordinates of vibration:

In-plane

$$\{\ddot{\xi}\} + 2\ \hat{\ell}[A]\{\dot{\xi}\} + \Big[(\hat{\ddot{\ell}}-\hat{\ell}^2)([I]+[A]) - (\hat{\Omega}^2[I]+[K])\Big]\{\xi\} = -\ \{f\} \tag{3a}$$

Out-of-plane

$$\{\ddot{\zeta}\} + 2\,\hat{\ell}[A]\{\dot{\zeta}\} + \Big[(\hat{\ddot{\ell}}-\hat{\ell}^2)([I]+[A]) - [K]\Big]\ \{\zeta\} = \{0\} \tag{3b}$$

with,

$$\{f\} = \left\{\frac{2}{\beta_k}\left(2\sigma_k\hat{\Omega}\hat{\ell} + \frac{T_4{}'}{\beta_k}\right)\right\}$$

$$[K] = (2[D]-[C])\,\hat{\ell}^2 + [D]\hat{\ddot{\ell}} - [C]\,\frac{T_1{}'}{2} + [I](T_5{}'+\hat{\ell}^2-\hat{\omega}_m^2) \tag{3c}$$

Comments

The final equations are seen to be coupled and non-autonomous hence, in general, are not amenable to any simple closed form solution. Both sets of equations are similar, with the in-plane result being slightly more involved. Rotation serves to reduce the effective stiffness for the in-plane case relative to out-of-plane motion. Also the in-plane degree of freedom experiences an additional loading resulting from the Coriolis force associated with deployment and rotation plus forces due to angular accelerations and the gravitational field. Deployment serves to alter stiffness while simultaneously introducing an effective positive damping. Type of trajectory is specified through $\dot{\theta}$ and eccentricity.

At a given point in time equation (3) is solved as a discrete eigenvalue problem. [A] being skew-symmetric implies eigenvalues and eigenfunctions exist in complex conjugate pairs. Frequency parameter will be constant in time only for the case of constant spin and no deployment, for which exact closed form solutions exist in the form of sinusoidal oscillation.

An exact numerical integration of the equations is used to generate system response data under some typical conditions.

3. Results and Discussion

Eigenvalues

From the time of orbital injection until steady state attitude equilibrium is achieved, a satellite can experience high rates of spin resulting in a very significant influence on flexible appendage characteristics. Figure 2 demonstrates this effect, for in-plane vibration, in an efficient and compact manner by plotting frequency parameter ($\beta_m^4 = \frac{\rho}{EI}\omega_m^2\ell^4$) over a large range of spin parameter values ($\lambda_s = \frac{\rho}{EI}\dot{\Omega}^2\ell^4$). Note that with newer generation spacecraft tending toward longer and longer members spin parameter values will also tend to be larger than in the past. Equations (3) are truncated so as to include only the first three modes. The relationship is essentially linear, i.e.,

$$\beta_m = k_m\,\lambda_s^{\frac{1}{4}} \tag{4}$$

There is no need to plot the out-of-plane result since comparing equations (3a) and (3b) for the case of 'free' vibration and spin only,

$$\beta_{m_o}^4 = \beta_{m_i}^4 + \lambda_s \tag{5}$$

Equation (5) is confirmed by the result of Table I. Note that these results allow one to vary frequency (ω_m), physical characteristics of the beam (ρ,EI,ℓ), and spin rate ($\dot{\Omega}$). The results point out the dramatic increase which could occur in frequency at spin-up/spin-down.

For booms aligned along the local radius vector $\underline{R}_c$, with lower values of the spin parameter ($0 \le \lambda_s^{\frac{1}{4}} \le 6$), the relationship with the in-plane frequency parameter is no longer linear - Fig. 3. Also, if the spin parameter results solely from orbital velocity frequencies are significantly higher than those resulting from pure spin when $\lambda_s > 1$. The reason for this is the dual effect of rotation to both stiffen and load the beam simultaneously while the gravity field tends to unload the beam. During orbiting-only conditions the gravitational field balances out the transverse loading effect of the beam - Eq. (3). A similar phenomenon exists for out-of-plane oscillations. The unstable nature of the orientation for a beam lying along a tangent to the orbit is also displayed in Figure 3.

Isolated in Figure 4 is the influence of deployment rate and deployment acceleration. Regardless of whether the beam is extending or retracting, a decrease occurs in frequency of vibration with an increase in rate of extension. For a given deployment velocity the tendency toward nonoscillatory behaviour increases for longer booms. The trend is similar for booms accelerating out from the spacecraft. However the system becomes stiffer during deceleration. Note that although deployment is capable of a significant influence its effect can be nullified by orbital effects alone.

Much of the information contained in Figure 5 is implicit in earlier results, nevertheless, it will serve to clarify some of the basic changes occurring in frequency itself as the beam extends. With $\omega_m^2 \propto \frac{1}{\ell^4}$ large variations are experienced up to about 200 meters. Spin stiffens the system considerably such that these large variations in frequency last only up to 100 meters at 2.0 rpm. In the absence of spin and/or orbital effects behaviour becomes nonoscillatory at shorter lengths with increasing extension rate.

The behaviour observed can be predicted in large measure simply by examining the equation for the case m = 1, for which,

$$A_{11} = \underline{0};\ C_{11} = \underline{2.39};\ D_{11} = \underline{1.57}$$

$$\beta_1 = \underline{1.875};\ \sigma_1 = \underline{0.73}$$

Substituting in equation (3a) results in an equation of the form

$$\ddot{\xi}_1 + \omega_1{}^2 \xi_1 = -1.5\, \dot{\Omega}\, \hat{\dot{\ell}} + 0.5\, T_4{}' \qquad (6)$$

a simple nonhomogeneous second order ordinary differential equation where,

$$\omega_1{}^2 = -0.57\, \hat{\dot{\ell}} - 2.75\, \hat{\dot{\ell}}^2 + 1.2\, T_1{}' - (\dot{\Omega}^2 + T_5{}' - 1666)^*$$

Vibration frequency, which is associated with the imaginary part of the system eigenvalue, is of prime importance. However, Table 1 demonstrates that the real part can also prove of interest during deployment. In this case it is nontrivial and, in fact, it can be greater than zero implying instability - or, by analogy, a positive damping. Increasing deployment velocity can decrease frequency (or eliminate it altogether) while increasing the magnitude of the real part. That spin restores stability is implied for example, by a beam deploying at 2 rpm for which all real parts of the eigenvalue become negative. Additional results allow one to judge combined effects of deployment velocity, deployment accleration, and spin.

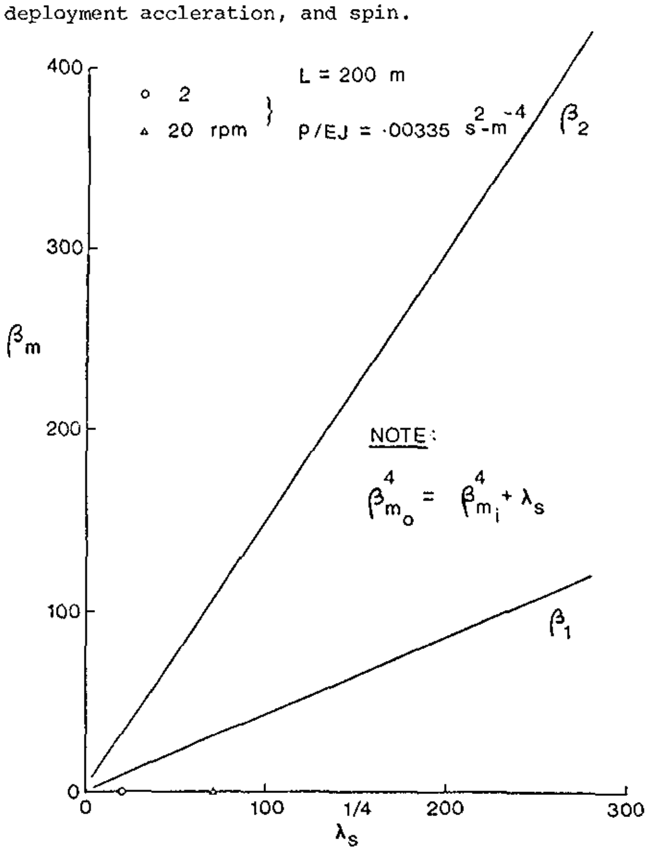

Fig. 2 Frequency parameter for in-plane vibrations covering a wide range of spin parameter values - no deployment.

*Based on ℓ = $\underline{36.576}$ m (Allouette II)
R_c = $\underline{6885}$ Km

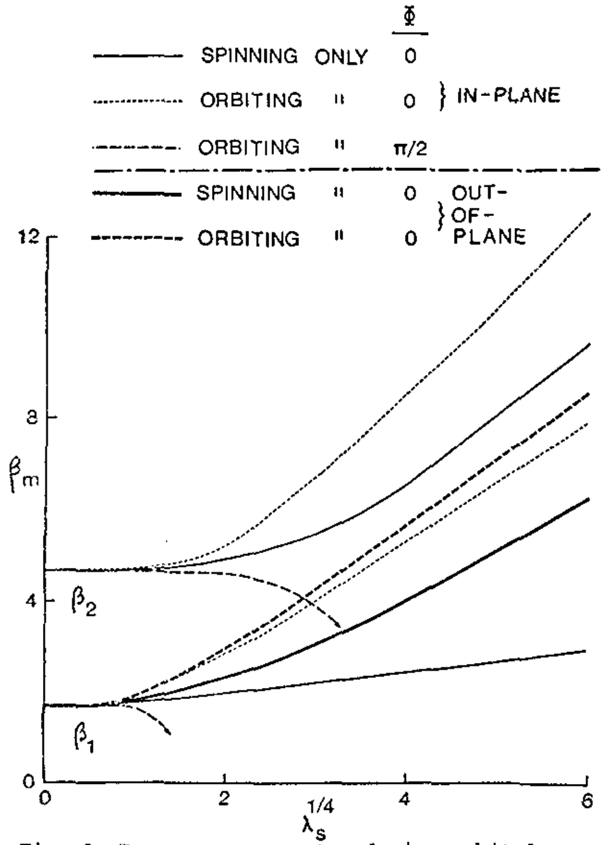

Fig. 3 Frequency parameter during orbital motion only (at differing appendage orientations) or spinning only, at small values of spin parameter and no deployment.

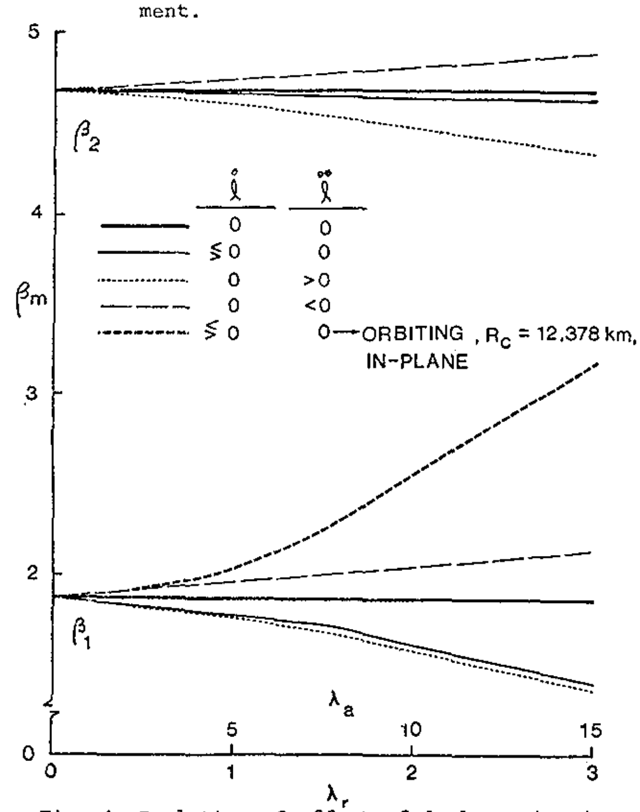

Fig. 4 Isolation of effect of deployment rate or deployment acceleration on frequency parameter.

Table 1. System Eigenvalues Demonstrating Individual and Combined Influences of Orbital Motion, Spin and Deployment†

SYSTEM	VIBRATION MODE	Φ	$\dot{\Omega}$, rpm	$\dot{\ell}$, m/s	$\ddot{\ell}$, m/s^2	EIGENVALUE REAL PART, 1/s 1st	EIGENVALUE REAL PART, 1/s 2nd	βm (BASED ON IMAGINARY PART OF EIGENVALUES) 1st	βm 2nd
Flexure Only	NA*	NA	0	0	0	0	0	1.875	4.694
Deploying	NA	NA	0	0.04	0	-0.395×10^{-7}	0.222×10^{-8}	1.869	4.693
	NA	NA	0	1.00	0	-0.134×10^{-1}	0.160×10^{-3}	0	4.087
	NA	NA	0	0	0.00001	0	0	1.874	4.693
	NA	NA	0	0	-0.00001	0	0	1.876	4.695
Orbiting ($\dot{\Phi}$ = 0)	In-Plane	0	$\dot{\theta}$	0	0	0	0	1.884	4.697
	In-Plane	π/2	$\dot{\theta}$	0	0	0	0	1.867	4.693
	Out-of-Plane	0	$\dot{\theta}$	0	0	0	0	1.887	4.697
	Out-of-Plane	π/2	$\dot{\theta}$	0	0	0	0	1.870	4.694
Spinning ($\dot{\theta}$ = 0)	In-Plane	0	0.2	0	0	0	0	2.336	5.991
	In-Plane	0	2.0	0	0	0	0	4.894	16.66
	In-Plane	0	20.0	0	0	0	0	15.15	52.58
	Out-of-Plane	0	0.2	0	0	0	0	3.647	6.155
	Out-of-Plane	0	2.0	0	0	0	0	11.12	17.41
	Out-of-Plane	0	20.0	0	0	0	0	35.14	54.95
Deploying	NA	NA	0	0.04	0.00001	-0.148×10^{-7}	0.839×10^{-9}	1.878	4.696
	NA	NA	0	0.04	-0.00001	-0.641×10^{-7}	0.359×10^{-8}	1.880	4.697
Deploying + Orbiting ($\dot{\Phi}$ = 0)	In-Plane	0	$\dot{\theta}$	0.04	0	-0.395×10^{-7}	0.222×10^{-8}	1.879	4.697
	In-Plane	0	$\dot{\theta}$	1.00	0	-0.140×10^{-1}	0.159×10^{-3}	0	4.092
	In-Plane	0	$\dot{\theta}$	0	0.00001	0	0	1.884	4.697
	In-Plane	0	$\dot{\theta}$	0	-0.00001	0	0	1.885	4.698
	In-Plane	0	$\dot{\theta}$	0.04	0.00001	-0.148×10^{-7}	0.839×10^{-9}	1.878	4.696
	In-Plane	0	$\dot{\theta}$	0.04	-0.00001	-0.641×10^{-7}	0.359×10^{-8}	1.880	4.697
	Out-of-Plane	0	$\dot{\theta}$	1.00	0	-0.140×10^{-1}	0.159×10^{-3}	0	4.092
Deploying + Spinning ($\dot{\theta}$ = 0)	In-Plane	0	2.0	0.04	0	-0.222×10^{-9}	-0.335×10^{-9}	4.894	16.66
	In-Plane	0	2.0	1.00	0	-0.348×10^{-5}	-0.524×10^{-5}	4.665	16.65
	In-Plane	0	2.0	0.04	0.00001	-0.833×10^{-10}	-0.126×10^{-9}	4.894	16.66
	In-Plane	0	2.0	0.04	-0.00001	-0.361×10^{-9}	-0.544×10^{-9}	4.894	16.66
	Out-of-Plane	0	2.0	1.00	0	-0.348×10^{-5}	-0.524×10^{-5}	11.10	17.39

*NA - Not Applicable

†R_c = 12,378 Km; e = 0; ℓ = 100 m; ρ/EJ = 0.00335 $\frac{s^2}{m^4}$

Eigenfunctions

Although data in Figures 6 and 7 have, in essence, been given in Reference 5 it is presented here for the sake of completeness and elaborated on further. Figure 6 clearly demonstrates that the stiffening effect of spin rate on eigenvalues extends as well to the eigenfunctions. Even at 2 rpm the effect is substantial with a limiting shape being reached by 10 rpm.

The stiffening behaviour of the eigenfunctions in Figure 7 is clearly due to the increase in length only and is not affected by deployment rate per se. It should be kept in mind, however, that eigenfunctions have been found altered by higher deployment rates (e.g. $\dot{\ell}$ = 1.0 m/s). Also, the effect of deployment is to produce sets of complex eigenfunctions. When evaluating Figures 6 and 7 one should bear in mind that for a simple non-deploying, non-rotating beam the shape of the eigenfunctions remains invariant with length.

Response

Boom response to an initial tip displacement equal to 5% of the length is displayed in Figure 8 by a plot of the generalized coordinate associated with the first admissible function (i.e. m = 1). The contribution of the second assumed mode was found to be null or << 5% in all situations. This is in part expected because of the nature of the initial condition, but it does support the conclusion stated in Reference 4 that modal coupling is negligible between the first two modes for deployment velocities of this order. Direct digital integration of equations (3a) - in-plane vibrations - provides the response data. The case of flexure only supplies a reference. Stiffening caused by spin is reflected by the increase in the oscillation frequency. No amplitude change occurs for such a conservative system. The deploying beam operates at a smaller amplitude because of the smaller initial length and hence smaller initial condition. It is deployment rate itself which shifts the frequency. Despite the smaller initial condition the deploying,

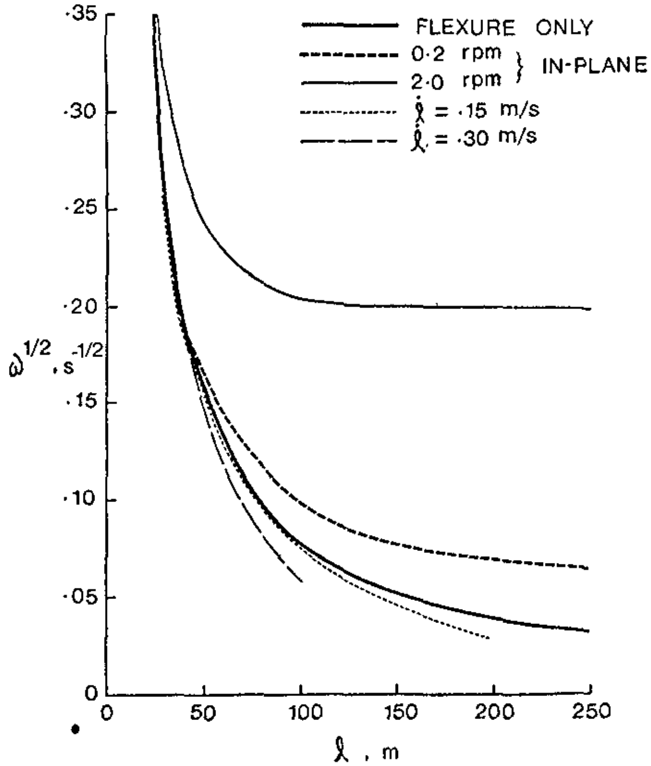

Fig. 5 Influence of changes in length, deployment rate, or spin rate on (in-plane) vibration frequency.

orbiting beam still experiences an increase in amplitude. This is a consequence of the Coriolis force contained in {f} - Eq. (3). In fact this amplitude increase is a prelude to the case of the deploying beam rotating at 2 rpm and experiencing nonlinear displacement. An order of magnitude check reveals that the $\dot{\Omega}\dot{\ell}$ term is capable of severely loading the boom. Although not shown here this effect could be either augmented or reduced by spin acceleration. Out-of-plane vibrations occur at a higher frequency, but do not experience the applied load {f} which causes the excessive displacements.

4. Conclusions

Presented is a method of solution for a deploying, orbiting, librating, beam-type spacecraft appendange capable of transverse oscillation both in and out of the plane of rotation. The object is to provide the reader with some appreciation as to the influence deployment and rotation parameters have either separately, or combined. Among the more salient observations are, that:

(1) An orbiting beam cannot be treated as simply a rotating beam because of the presence of the gravitational field which can contribute to higher frequencies, depending on the relative magnitude of spin libration.

(2) The 'free' vibration characteristics of out-of-plane motion during spin is identical with in-plane motion except that it occurs at a higher frequency (Eq. (5)).

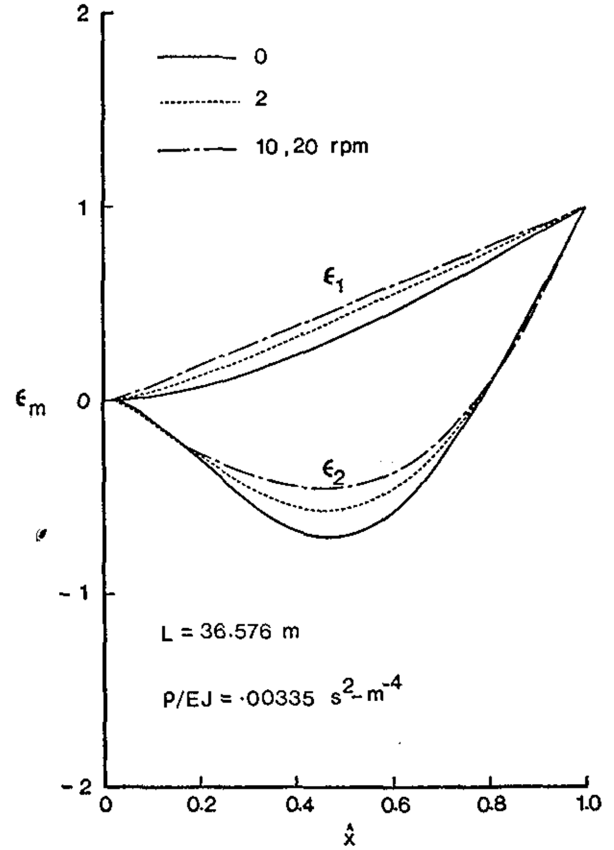

Fig. 6 Spin rate and its influence on system eigenfunctions in the absence of deployment.

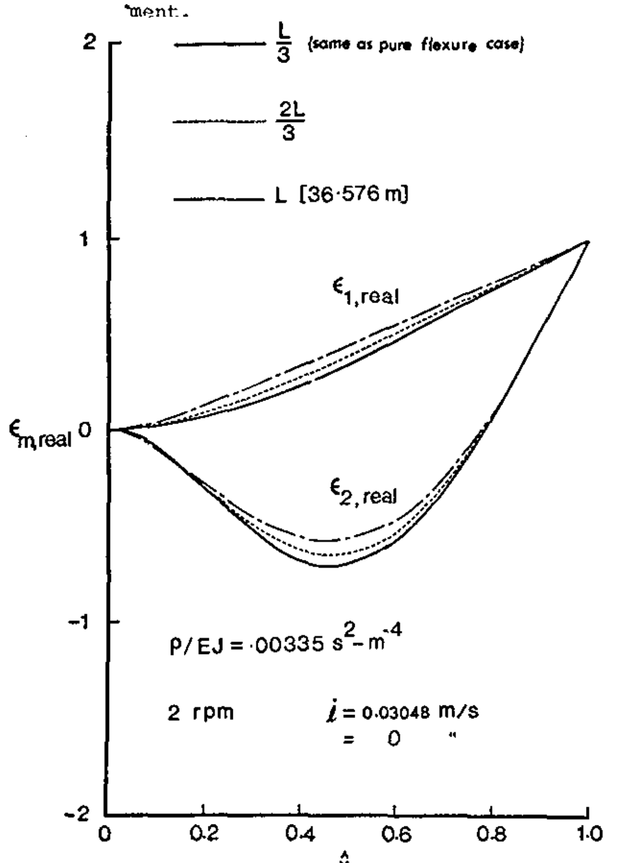

Fig. 7 Mode changes associated with changes in length of a spinning deploying beam.

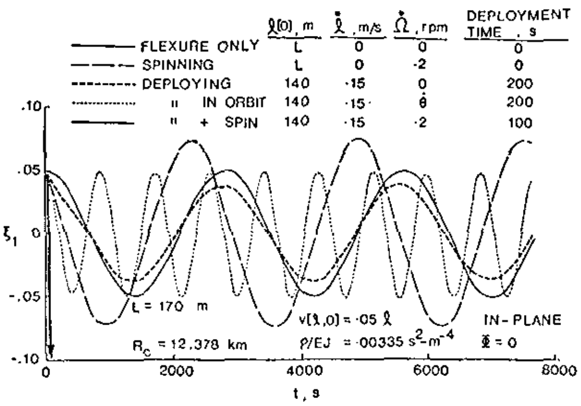

Fig. 8 Response of deploying, rotating, beam-type appendage to initial tip displacement.

(3) In the absence of rotation deployment rate introduces instability into the system regardless of the direction of extension. Similar behaviour results from acceleration of the boom out from the spacecraft and vice-versa during deceleration.

(4) The changing of length itself as opposed to deployment rate or change in deployment rate remains one of the strongest factors influencing frequency variations during deployment (spinning or non-spinning).

(5) Spin accelerations do not affect system eigenvalues or eigenfunctions but, rather, contribute an additional transverse load on the beam.

(6) Rate of rotation plays a dominant role in stiffening the system as evidenced by the sizeable increase in spin parameter and by the straightening of the eigenfunctions (Figs. 2,3,5,6) at higher spin rates.

(7) Orbital effects can be dealt with primarily through the spin parameter.

(8) Deployment-related Coriolis forces play a major role in causing large in-plane deformations. This tends to limit the amount of time which can be allowed any given stage of the deployment process.

(9) The method of analysis allows considerable insight to be had into the interactions of the many and varied parameters involved. This is made possible by the similarity of the generalized coordinate equations to those governing single degree of freedom mass-spring-damper motion in classical vibration theory.

Results presented apply to both spinning and gravity-gradient spacecraft both during and after attitude acquisition. The frequency parameter data should be useful in dealing with problems of interactions between the structural, control, and vehicle dynamics.

This work represents a preliminary step in analyzing a complex phenomenon of importance to present and future space ventures.

References

1. Modi, V.J., "Attitude Dynamics of Satellites with Flexible Appendages - A Brief Review", Journal of Spacecraft and Rockets, Vol. 11, No. 11, November 1974, pp. 743-751.

2. Likins, R.W., et al., "Mathematical Modelling of Spinning Elastic Bodies for Modal Analysis", AIAA Journal, Vol. 11, No. 9, September 1973, pp. 1251-1258.

3. Tabarrok, B., et al., "On the Dynamics of an Axially Moving Beam", Journal of the Franklin Institute, Vol. 297, No. 3, March 1974, pp. 201-220.

4. Jankovic, Miodrag S., "Lateral Vibrations of an Extending Rod", University of Toronto Institute for Aerospace Studies, Technical Note No. 202, April 1976.

5. Lips, K.W., and Modi, V.J., "Transient Attitude Dynamics of Satellites with Deploying Flexible Appendages", XXVIII International Astronautical Congress, Praha, Czechoslovakia, September 1977, Paper No. 77-225.

6. Kaza, K.R.V., and Kvaternik, R.G., "Nonlinear Flag-Lag-Axial Equations of a Rotating Beam", AIAA Journal, Vol. 15, No. 6, June 1977, pp. 871-874.

7. Cherchas, D.B., and Gossain, D.M., "Dynamics of a Flexible Solar Array During Deployment from a Spinning Spacecraft", CASI Transactions, Vol. 7, No. 1, March 1974, pp. 10-18.